COBEM 2023 27TH INTERNATIONAL CONGRESS OF MECHANICAL ENGENEERING

ABCM Brazilian Society of Mechanical Sciences and Engineering
27th ABCM International Congress of Mechanical Engineering
December 04-08, 2023, Florianópolis-SC, Brazil

COBEM2023-0320 TOPOLOGY OPTIMIZATION OF COMPLIANT MECHANISMS SUBJECTED TO HARMONIC LOADS

Valéria Farias da Luz
Universidade do Estado de Santa Catarina. R. Paulo Malschitzki, 200 - Zona Industrial Norte, Joinville - SC, Brazil. Zip code: 89219-710

Olavo M. da Silva Junior
Acoustics and Vibration Lab., Federal University of Santa Catarina (UFSC), Trindade, Florianópolis - SC, Brazil. Zip code: 88040-900

Eduardo Lenz Cardoso
Universidade do Estado de Santa Catarina. R. Paulo Malschitzki, 200 - Zona Industrial Norte, Joinville - SC, Brazil. Zip code: 89219-710

Abstract. *Compliant mechanisms are used to modify kinematic and/or kinetic relationships, through the connection between actuators (inputs) and receivers (output) by elastic deformation of the mechanism. In view of the complexity of its geometry, topology optimization is generally used to design a compliant mechanism from scratch. This work proposes a new formulation to design compliant mechanisms subjected to harmonic loads, where the objective is to maximize the harmonic amplitude of the output displacements while constraining input displacements, volume and local harmonic stresses. The Augmented Lagrangian method is used to convert the original constrained problem into an equivalent unconstrained optimization, due to large number of local stress constraints. QP relaxation is used to avoid singularities in stress parameterization and spatial filtering and non-linear projection are used for complexity control. Analytical sensitivities are obtained using the adjoint approach to harmonic equilibrium equations. In this work, the design of an inverter mechanism is used to study the proposed formulation. The results shown the influence of excitation frequency on the topology.*

Keywords: *Compliant mechanisms, Topology optimization, Harmonic loads.*

1. INTRODUCTION

Contemporary works designing compliant mechanism using Topology Optimization (topopt) differ according to the formulation used in their objective function. Some use the kinematic approach, such as Borovinšek *et al.* (2020), Pereira and Cardoso (2018), Cai *et al.* (2023), Liang *et al.* (2020), Lu and Tong (2021), Nejat, Ali; Held, Alexander; Seifried (2022), where the objective function is obtained through relations between stiffness and flexibility of the inputs and outputs of the mechanisms. Other works use energy based formulations, where the compliant mechanism is considered as an energy transformation device. This transformation takes place from the input forces arising from the external environment that are converted into some output. Such operation must be performed in order to maximize the effective energy, which is the energy conversion efficiency of the mechanism (Miyajima *et al.* (2022), Ding *et al.* (2021), Zhu *et al.* (2020) and Cardoso and Fonseca (2004)).

The vast majority of works in the literature address the static regime ((Kang *et al.*, 2001), (Jung and Park, 2015), (Lee and Park, 2015), (Park, 2010)), however, work considering the dynamic regime has been growing over the last few years ((Venini, 2016), (Yang and Li, 2012), (Yang and Li, 2013) and (Zhu *et al.*, 2017)). According to Montero *et al.* (2020) there is no single methodology used for the topology optimization of dynamic problems, whether modal, harmonic or transient. Harmonic analysis, the object of the present study, is used when one wants to obtain the steady-state response of a structure subject to periodic loading.

The study of topology optimization considering harmonic loads began with Ma *et al.* (1993), where the concept of dynamic flexibility was introduced. Although this concept is a direct extension of the well known static compliance, there are some problems with this measure in the presence of anti-resonances in the frequency spectrum and the instability of the derivatives when the harmonic frequency is the same as the resonance frequency (Montero *et al.*, 2020).

Min *et al.* (1999) used an average minimum dynamic flexibility value for different frequencies. Tcherniak (1999) revealed the occurrence of discontinuity problems when using only the dynamic flexibility, so it was necessary to apply the static flexibility as a design constraint. This work also introduced an external buffer to avoid the disconnection between structures.

Montero *et al.* (2020) proposed the use of a weighted density norm to avoid many shortcomings associated to the dynamic compliance. Silva (2017) linked dynamic flexibility to input power functions to design resonant structures.

In addition to the way of quantifying the harmonic response, the purpose of using the designed component is also a

dividing factor between the works. The use of harmonic loads allows the design of structures for two different purposes: suppression of the oscillatory response (minimization of the frequency response, as in Shu *et al.* (2011) and resonant structures (maximization of the frequency response) as in Montero *et al.* (2020). Both approaches modify the structure as its resonant frequency approaches or moves away from the imposed excitation frequency.

1.1 Harmonic Analysis

The mechanical behavior of a a continuous medium comprised of linear elastic materials can approximately described by a coupled system of second-order ordinary differential equations

$$\mathbf{M}\ddot{\mathbf{U}}(t) + \mathbf{C}\dot{\mathbf{U}}(t) + \mathbf{K}\mathbf{U}(t) = \mathbf{F}(t), \tag{1}$$

where $\mathbf{M}$ is the global mass matrix, $\mathbf{C}$ is the global damping matrix, $\mathbf{K}$ is the global stiffness matrix, $\mathbf{U}$ is the global displacement vector and the dots refer to time derivatives. In this work, this system is obtained by using the Finite Element method, as detailed by Valentini *et al.* (2021). The global damping matrix is considered to be a linear combination on the form

$$\mathbf{C} = \alpha\mathbf{M} + \beta\mathbf{K}, \tag{2}$$

also known as proportional damping or Rayleigh damping, were α and β are used defined material parameters.

Consider a structure with a linear response excited by a set of harmonic forces, such that the amplitude varies over time according to a fixed angular frequency ω, in the form

$$\mathbf{F}(t) = \mathbf{F}_0 e^{i\omega t}, \tag{3}$$

where $\mathbf{F}_0$ is the force vector containing the amplitudes and i is the complex component $\sqrt{-1}$. Based on the assumption of linearity of the system and considering that the response due to the initial conditions has already dissipated, the response of the permanent displacements can be written as

$$\mathbf{U}(t) = \mathbf{U}_0 e^{i\omega t}, \tag{4}$$

where $\mathbf{U}_0$ is the global amplitude displacement vector.

Velocity and acceleration are the first and second derivatives of Eq. (4), respectively

$$\dot{\mathbf{U}}(t) = i\omega\mathbf{U}_0 e^{i\omega t}, \tag{5}$$

and

$$\ddot{\mathbf{U}}(t) = -\omega^2\mathbf{U}_0 e^{i\omega t}. \tag{6}$$

Substituting these expressions into the global equilibrium equation, Eq. (1), we arrive at

$$\left(-\omega^2\mathbf{M} + i\omega\mathbf{C} + \mathbf{K}\right)\mathbf{U}_0 e^{i\omega t} = \mathbf{F}_0 e^{i\omega t}, \tag{7}$$

or

$$\mathbf{K_D}\mathbf{U}_0 = \mathbf{F}_0, \tag{8}$$

with

$$\mathbf{K_D} = -\omega^2\mathbf{M} + i\omega\mathbf{C} + \mathbf{K}, \tag{9}$$

called the dynamic stiffness matrix. Thus, the displacements $\mathbf{U}_0$ at a given angular frequency ω can be obtained by solving the linear system of equations of Eq. (7). This vector is complex, with the real part representing the displacement amplitude and the imaginary part its phase.

The Cauchy stress tensor used in this work considers an additional viscous term

$$\boldsymbol{\sigma} = \mathbf{D} : \boldsymbol{\varepsilon} + \beta\mathbf{D} : \dot{\boldsymbol{\varepsilon}}, \tag{10}$$

where $\mathbf{D}$ is the constitutive tensor of the elastic linear material, $\boldsymbol{\varepsilon}$ is the tensor of infinitesimal deformations at the point, $\dot{\boldsymbol{\varepsilon}}$ is the its rate of change (Montero *et al.*, 2019). This viscous stress can be evaluated at a superconvergent point k of a finite element e as

$$\boldsymbol{\sigma}_{e,k} = \mathbf{D}_{e,k}\mathbf{B}_{e,k}\mathbf{H}_e(\mathbf{U}_0 + i\beta\omega\mathbf{U}_0), \tag{11}$$

where $\mathbf{D}_{e,k}$ is the constitutive matrix of the material at point k of element e, $\mathbf{B}_{e,k}$ is the matrix of derivatives of interpolation functions and $\mathbf{H}_e$ is a global-local transformation matrix for element e.

2. TOPOLOGY OPTIMIZATION AND MATERIAL PARAMETERIZATION

In general, optimization consists of extremizing a functional $f(\mathbf{x})$, dependent on a set of design variables $\mathbf{x}$ with side constraints $\underline{\mathbf{x}}$ and $\bar{\mathbf{x}}$ and subjected to a set of functional constraints g_i

$$\begin{cases} \min & f(\mathbf{x}), \\ S.t. & \\ & g_i(\mathbf{x}) \leq \overline{g}_i \\ & \underline{\mathbf{x}} \leq \mathbf{x} \leq \bar{\mathbf{x}} \end{cases}. \tag{12}$$

When the quantities and variables involved in the formulation are associated with a structural problem, it is common to refer to the optimization process as structural optimization.

Topology structural optimization is a method that aims at the distribution of material in a fixed design domain. This material distribution is usually represented by the set of variables $\boldsymbol{\rho}$, known as relative densities, associated with the material properties of a base isotropic material at each point of its domain.

Mesh dependence is both a physical and a mathematical problem, as it is known that the optimal solution for the distribution of an isotropic material consists of creating infinitesimal reinforcements. Therefore, the more refined the discretization by finite elements, for example, the greater the number of design variables and the smaller the size of the reinforcements that the optimizer will create. In these cases, spatial filters are used to impose (even if only approximately) a scaling control to prevent the optimization from creating reinforcements smaller than the filtering radius. In general, we can indicate this operation as a mapping between a set of variables $\mathbf{x}$ (also called mathematical variables) to a set of filtered variables $\tilde{\boldsymbol{\rho}}$

$$\mathbf{x} \overset{Filter}{\rightarrow} \tilde{\boldsymbol{\rho}}. \tag{13}$$

However, the fact that we use filters and also a continuous parameterization of material means that the optimal solution contains many design variables with intermediate value. The most used solution in the literature consists of using some smooth approximation for the Heaviside operator, such that the optimized relative densities assume values 0 or 1. This operation is usually called projection and is performed after the filtering step, such that

$$\mathbf{x} \overset{Filter}{\rightarrow} \tilde{\boldsymbol{\rho}} \overset{Projection}{\rightarrow} \boldsymbol{\rho} \tag{14}$$

where $\boldsymbol{\rho}$ are the relative densities that will be used to describe the distribution of the material.

The spatial filter used evaluates $\tilde{\boldsymbol{\rho}}$ for a given element e through the weighted average of the $\mathbf{x}$ defined in the neighborhood Ω_e of the elements and the relative weights $w_{e,i}$

$$\tilde{\rho}_e = \frac{\sum\limits_{i \in \Omega_e} w_{e,i} x_i}{\sum\limits_{i \in \Omega_e} w_{e,i}}. \tag{15}$$

The neighborhood Ω_e is defined as the set of elements inside a given radius R, such that

$$\Omega_e = \{i \mid d_{i,e} \leq R\} \tag{16}$$

where $d_{i,e}$ is the distance between the centroids of elements e and i. The relative weights are defined by

$$w_{e,i} = 1 - \frac{d_{i,e}}{R}. \tag{17}$$

The projection used in this work is the smooth approximation of the Heaviside function

$$\rho_e = H(\tilde{\rho}_e - \eta) \approx \frac{\tanh \beta_f \eta + \tanh \beta_f (\tilde{p}_e - \eta)}{\tanh \beta_f \eta + \tanh \beta_f (1 - \eta)} \tag{18}$$

where $\eta = 0.5$ is the value where the transition between 0 and 1 must occur and β_f is an adjustment factor of the Heaviside approximation (Wang *et al.*, 2011). The higher the value of β_f, the closer to the real Heaviside.

2.1 Material Parametrization

During the topology optimization, some elements may present low values of relative densities (voids) and can generate localized artificial vibrations due to the artificially high mass/stiffness ratio (Neves *et al.*, 1995).

Olhoff and Du (2008) proposed an approach for mass parametrization

$$\mathbf{M}_e = \begin{cases} (\rho_l + (1-\rho_l)\rho_e)\mathbf{M}_e^0, \text{se } \overline{\rho} < \rho_e \leq 1.0 \\ (\rho_l + (C_1\rho_e^6 + C_2\rho_e^7))\mathbf{M}_e^0, \text{se } \rho_e \leq \overline{\rho}, \end{cases} \tag{19}$$

where $\mathbf{M}_e^0$ is the mass matrix of element e with no parametrization, ρ_l is the minimum value for ρ, $\bar{\rho}$ is a transition value, and C_1 and C_2 are given by

$$C_1 = -\frac{6\rho_l - 6}{\overline{\rho}^5} \tag{20}$$

and

$$C_2 = -\frac{5\rho_l - 5}{\overline{\rho}^6}. \tag{21}$$

A value of $\bar{\rho} = 0.1$ is used in this work. The traditional Solid Isotropic Material with Penalization (SIMP) is used to parameterize the stiffness

$$\mathbf{K}_e = \rho_e^P \mathbf{K}_e^0, \tag{22}$$

where $\mathbf{K}_e^0$ it the stiffness matrix of element e with no parametrization.

2.2 Stress constrain

Stress analysis is essential for flexible mechanisms as it avoids designing a structure that does not support the applied dynamic loads. However, its application presents two difficulties: the fact that the stress is a local measure (dimension problem) and irregular feasible solution space (singularity problem).

The high number of constraints makes it difficult to use local constraints in traditional optimizers as it implies a high computational time and increased instability in the solution (Pereira and Cardoso, 2018). Mitigation of the dimensionality problem can be accomplished through the use of aggregation strategies (such as regional norms and constraints), targeting a small number of constraints, or by using the Augmented Lagrangian method (Valentini *et al.*, 2021).

The irregular design space associated to stress constraints was first addressed by Svéd and Ginos (1968) and was further investigated by Kirsch (1989, 1990). The extension to continuum problems was given by Duysinx and Bendsøe (1998), motivating the QP relaxation proposed by Bruggi (2008). In essence, the original stress parametrization leads to the situation where the optimizer cannot remove material to satisfy the stress constraints, leading to topologies comprised of many intermediate relative densities.

The QP relaxation is given by

$$\boldsymbol{\sigma}_{e,k} = \rho_e^{P-Q}\boldsymbol{\sigma}_{e,k}^0, \tag{23}$$

where $\boldsymbol{\sigma}_{e,k}^0$ is the nominal stress, P is the exponent used for the SIMP parametrization and $Q < P$ is a relaxation exponent.

3. FORMULATION

This section aims to present the proposed formulation applicable to a flexible inverter mechanism.

In a static problem, the goal of an inverter mechanism is to maximize the (negative) output displacement u_{out} by relative to an input force

$$P \begin{cases} \min \quad -u_{out}(\mathbf{x}), \\ S.t. \\ \quad \mathbf{K}(\mathbf{x})\mathbf{U}(\mathbf{x}) = \mathbf{F} \\ \\ \quad u_{in}(\mathbf{x}) \leq \bar{u}_{in} \\ \quad \sigma_{e,k}(\mathbf{x}) \leq \bar{\sigma} \\ \quad V(\mathbf{x}) \leq \bar{V} \\ \quad \underline{\mathbf{x}} \leq \mathbf{x} \leq \bar{\mathbf{x}} \end{cases} \tag{24}$$

where u_{out} is the output displacement, u_{in} is the input displacement, $\sigma_{e,k}$ is the equivalent von-Mises stress at super-convergent point k of element e, V is the volume, $\bar{V}$ is the limit volume, $\bar{\sigma}$ is the limit stress and $\bar{u}_{in}$ is the limit input displacement.

However, in an harmonic system, the displacement value has real and imaginary parts,

$$u = u_R + iu_I, \tag{25}$$

and therefore, one cannot simply use the output displacement as it has two values: magnitude and phase. Although the use of the absolute value is a possibility, it hinders the signal (direction) of the displacement. Also, the inversion means that the output displacement must be opposite to the input displacement, an obvious requirement for static problems. Nonetheless, it is known that harmonic problems can show phase inversion, specially when passing through a resonance. Therefore, the objective function was modified, aiming to combine the maximization of the output displacement with the phase inversion at exactly 180° with respect to the input displacement. The new formulation reads

$$P\begin{cases} \max & -\frac{\Re(u_{out}(\mathbf{x}))}{\Re(u_{in}(\mathbf{x}))} \\ S.t. & \\ & \mathbf{K_D}(\mathbf{x})\mathbf{U}_0(\mathbf{x}) = \mathbf{F}_0 \\ & |u_{in_j}(\mathbf{x})| \leq \bar{u}_{in_j} \qquad j = 1..n_{uin} \\ & \sigma_{e,k}(\mathbf{x}) \leq \bar{\sigma} \qquad e = 1..n_e\,,\ k = 1..n_k \\ & V(\mathbf{x}) \leq \bar{V} \\ & \underline{\mathbf{x}} \leq \mathbf{x} \leq \bar{\mathbf{x}} \end{cases} . \tag{26}$$

Constraints are written in their normalized form as

$$g_{in_j}(\mathbf{x}) = \frac{|u_{in_j}(\mathbf{x})|}{\bar{u}_{in_j}} - 1, \tag{27}$$

$$g_{vm}(\mathbf{x}) = \frac{V(\mathbf{x})}{\bar{V}} - 1 \tag{28}$$

and

$$g_{\sigma}(\mathbf{x}) = \frac{\sigma_{e,k}(\mathbf{x})}{\bar{\sigma}} - 1, \tag{29}$$

where the absolute value $|a| = \sqrt{\Re(a)^2 + \Im(a)^2}$ of the input displacements are used. The equivalent stress for harmonic problems can be written as

$$\sigma_{e,k} = \sqrt{\boldsymbol{\sigma}_{e,k}^H \mathbf{V} \boldsymbol{\sigma}_{e,k}}, \tag{30}$$

where $\boldsymbol{\sigma}_{e,k}^H$ is the complex conjugate of $\boldsymbol{\sigma}_{e,k}$ and $\mathbf{V}$ is the Voigt matrix.

The Augmented Lagrangian method (LA) was chosen to address the large number of functional constraints (da Silva *et al.*, 2018). The modified problem is written as

$$P^k\begin{cases} \min & \mathcal{L}(\mathbf{x}) = f(\mathbf{x}) + \sum_n \mathcal{L}_{g_n}(\mathbf{x}) \\ & \underline{\mathbf{x}} \leq \mathbf{x} \leq \bar{\mathbf{x}} \end{cases} \tag{31}$$

where $f(\mathbf{x})$ is the objective function and each $\mathcal{L}_{g_n}(\mathbf{x})$ is given by

$$\mathcal{L}_{g_n}(\mathbf{x}) = \frac{c^k}{2}\left\langle \frac{\mu_n^k}{c^k} + g_n(\mathbf{x}) \right\rangle^2 . \tag{32}$$

where c^k is a penalty and μ_n^k are multipliers associated to each constraint n. Super index k represents the external iteration used to adjust the penalty and the multipliers (da Silva *et al.*, 2018). A modified steepest descent with projection was used to solve each problem P^k (Cardoso and Heiden, 2023).

According to Montero *et al.* (2020), sensitivity analysis of Eq. (31) can be evaluated as

$$\frac{d\mathcal{L}}{dx_m} = \frac{\partial \mathcal{L}}{\partial x_m} + \Re\left(\boldsymbol{\lambda}^T \frac{d\mathbf{K}_D}{dx_m}\mathbf{U}\right) - 2\Re\left(\frac{d\mathbf{F}}{dx_m}\right) \tag{33}$$

where $\boldsymbol{\lambda}$ is obtained by solving an adjoint problem

$$\mathbf{K}_D\boldsymbol{\lambda} = \left(i\frac{\partial \mathcal{L}}{\partial \mathbf{U}_I} - \frac{\partial \mathcal{L}}{\partial \mathbf{U}_R}\right), \tag{34}$$

where $\mathbf{U}_R$ and $\mathbf{U}_I$ are, respectively, the real and complex parts of the displacement vector.

3.1 Damping model and continuation

One problem with the topology optimization of continuum structures subjected to harmonic loads and the use of the proportional damping is the fact that the damping varies with the stiffness and mass. Thus, for each change in topology, there is a subsequent change in damping. According to Silva (2017), it is possible to use a particular form of proportional damping to make the effective damping independent of the topology. In this form, also known as structural damping, the damping coefficient α is null and the coefficient associated to the stiffness is given by

$$\beta = \frac{\zeta}{2\omega} \tag{35}$$

where ζ is a given damping ratio and ω is the angular frequency of the excitation. Another problem when addressing harmonic problems is the presence of resonances. When the optimization passes through a resonance and the damping ratio is small, on can observe some numerical problems due to the large condition number of the dynamic stiffness matrix, Eq. (9). Therefore, Valentini *et al.* (2021) proposes the use of a continuation approach, where the damping ratio starts with a large number ($\zeta_{ini} = 0.3$, for example) and decreases at each external iteration of the LA procedure until the target value ζ_{fin}.

4. RESULTS AND CONCLUSIONS

Topology optimization in the harmonic regime is highly influenced by the angular excitation frequency ω. Also, contrary to the traditional static formulation, the harmonic problems depends on more factors, like mass, damping and how close the excitation frequency is to the resonances.

In order to understand the influence of excitation frequency in the optimized topology of an inverter mechanism under harmonic regime, some studies were carried out and the results are presented in this section.

The geometry and the boundary conditions are shown in Fig. 1, with values given in Tab. 1. Distributed input forces and output stiffness are used to avoid stress concentrations in the input and in the output regions. Nonetheless, just one DOF was used to evaluate the input (horizontal displacement in the lower left corner) and just one DOF as used to evaluate the output displacement (horizontal displacement in the lower right corner). The relative density of some elements were kept fixed in 1 (full base material) and are indicated as black in Fig. 1. The initial value for all design variables is also 1.

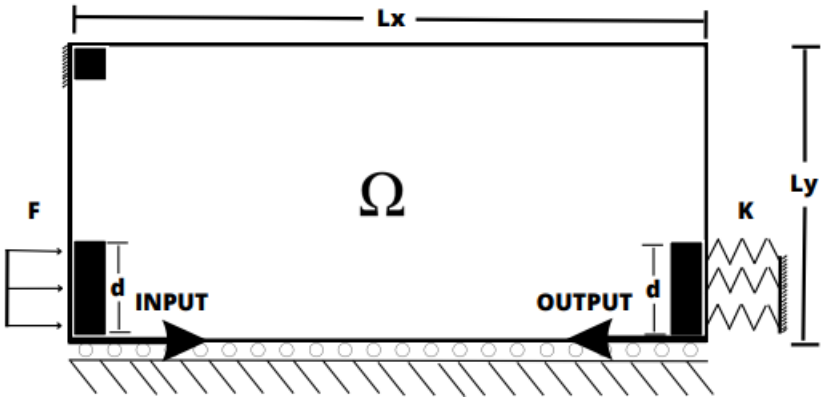

Figure 1. Inverter mechanism: geometry and boundary conditions.

The material properties and constraint values were based on Pereira and Cardoso (2018) and are shown in Table 2.

The number of external iterations for the LA, the number of internal iterations for the modified steepest descent and the initial and final value for the damping ratio are shown in Tab. 3.

Table 1. Geometry and mesh parameters.

Variable	Value	Description
nx	60	Divisions along the length
ny	30	Divisions along the width
Lx	100 cm	Domain Length
Ly	50 cm	Domain Width
Lz	0.5 cm	Domain Thickness
d	0.5 cm	Dimension of filled region

Table 2. Fixed parameters.

Variable	Value	Description
E	$3.0 \times 10^9 Pa$	Young's Modulus
ν	0.4	Poisson coefficient
F_{in}	40×10^3 N/m	Distributed input force
K_{out}	1.0×10^5 N/m	Distributed stiffness in output
$\bar{u}_{in}$	2.0×10^{-3} m	Limit input displacement
$\bar{v}$	0.25	Limit volume fraction
$\bar{\sigma}$	30×10^6 Pa	Limit equivalent stress
P	3.0	SIMP exponent
Q	1.5	Stress relaxation exponent

Table 3. Parameters used in the optimization.

Variable	Value	Description
n_k	15	Number of external iterations in the LA
n_{int}	500	Number of internal iterations in the optimizer
ζ_{ini}	0.3	Initial value for the damping ratio (ζ)
ζ_{fin}	0.02	Target value for ζ
R	2.5 mm	Filter radius

A first analysis was performed for a null excitation frequency (equivalent to the static case), as shown in the first row of Table 5. The first natural frequency of this design is 452 Hz.

Some tests were performed to analyze the influence of the excitation frequency on the optimized designs. The study was performed for a frequency range in $[0, 900]$ Hz, approximately twice the value of the first natural frequency at 0 Hz. Table 5 presents the topology, equivalent stress distribution and first natural mode for each analyzed case.

It can be seen that the topologies obtained for excitation frequencies in the range 0 to 600 Hz are similar, with notable differences close to the output region (it gets thicker). Another interesting aspect is the opposite behavior in the region close to the input, as it gets thinner. The topology for 700 Hz is different as it has an additional reinforcement. The topology for 800 Hz suffers from disconnection between the input and the output, a known problem for harmonic problems at higher frequencies (Silva, 2017).

The fact that the region close to the input gets thinner can be linked to the last column of Table 5, since the vibration mode gets more and more localized close to the input as the frequency increases. The first natural frequency for the 800 Hz case is a rigid body mode, since the masses at the input and the output are disconnected.

Another important set of information regarding the optimized results shown in Tab. 5 is the type and the number of active constraints. It can be seen that the input displacement constraint is always active at the optimum, unlike the volume and the local stress constraints. Also, the number of active stress constraints is very low. Those few elements are the darker elements in the third column of Tab. 5 and are usually close to the most flexible part of the mechanism, as expected.

Table 6 shows another interesting fact regarding the physical mechanism used by the optimization procedure, as it can be seen that the optimization is pushing the first natural frequency to the right of the excitation frequency. The second and the third natural frequencies are also being pushed to the right of the spectrum.

The last column of Tab. 4 shows the objective function at the optimized point. It can be seen that the geometric advantage is quite low for 500 Hz and 700 Hz and attains the largest value for the 100 Hz design. Again, from the second column of Tab. 5, it is clear that the 100 Hz design has two regions with lumped flexibility, leading to a more efficacy. Another clue on the superior performance of this design can be seen on the last column of Tab. 5, since the vibration mode has a more widespread (global) pattern, linking the input to the beginning of the output region.

Table 4. Active constraints and goal value

Frequency	g_{in}	g_{vm}	g_{σ}	Objective function
0 Hz	Active	Active	-	7.94×10^{-2}
100 Hz	Active	Active	Active (2)	9.36×10^{-2}
300 Hz	Active	Active	Active (2)	7.72×10^{-2}
600 Hz	Active	-	Active (1)	1.16×10^{-2}
700 Hz	Active	Active	-	5.16×10^{-3}

Table 5. Optimized topology, equivalent stress distribution and first natural mode as the excitation frequency is changed. The term inside the parenthesis, f_1 is the first natural frequency for the optimized design.

Frequency (f_1)	Topology	Equivalent Stress	1° vibration mode
0 Hz (452 Hz)	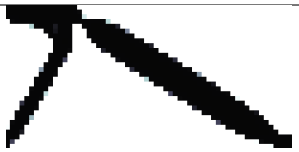		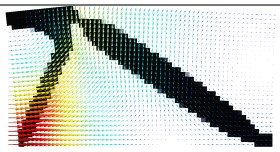
100 Hz (380 Hz)			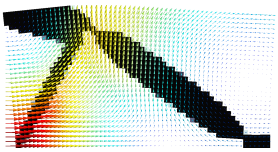
300 Hz (456 Hz)			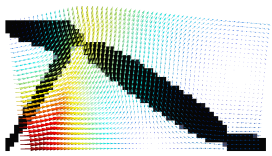
600 Hz (784 Hz)		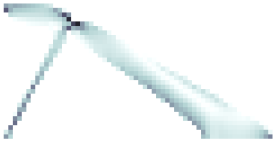	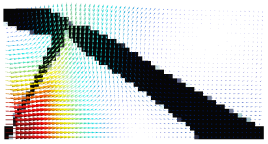
700 Hz (989 Hz)			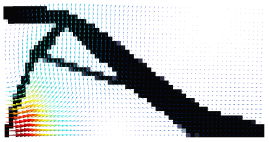
800 Hz (0.4 Hz)			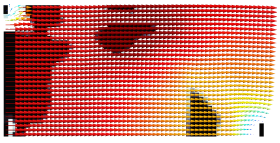

Table 6. Fist three natural frequencies for the optimized topology at each excitation frequency.

Frequency (Hz)	f_1 (Hz)	f_2 (Hz)	f_3 (Hz)
0	452	1319	2555
100	380	1582	2458
300	456	1797	2398
600	784	1843	2305
700	989	2021	2681

5. CONCLUSIONS

This work addressed the optimal design of compliant mechanisms under harmonic excitations. The objective was the maximization of the ratio between the real part of the output displacement to the real part of the input displacement, and the design of an inverter mechanism was used as example. Local harmonic stress constraints were also considered along an input displacement constraint and the traditional volume constraint. The Augmented Lagrangian technique was used to aggregate all the constraints in an equivalent unconstrained problem. Results show that the excitation frequency plays a very important role in the design and that the optimization pushes the first natural frequency of the design to the right of the excitation frequency. Patterns in the optimized solutions could be identified and can be used to enhance the formulation. The design for 800 Hz (and above) suffer from a well known problem in the topology optimization under harmonic regime - the disconnection between forces and the supports. It seems to be worst in the design of compliant mechanisms under harmonic regime, since there is also disconnection between the input and the output. Further investigations are needed to improve the formulation for higher excitation frequencies.

6. ACKNOWLEDGEMENTS

Authors acknowledge CNPq (process number 303900/2020-2) and FAPESC (process numbers 2021TR843 and 2023 TR000563). This study was financed in part by the Coordenação de Aperfeiçoamento de Pessoal de Nível Superior - Brasil (CAPES) - Finance Code 001.

7. REFERENCES

Borovinšek, M., Novak, N., Vesenjak, M., Ren, Z. and Ulbin, M., 2020. "Designing 2D auxetic structures using multi-objective topology optimization". *Materials Science and Engineering A*, Vol. 795, No. March. ISSN 09215093. doi:10.1016/j.msea.2020.139914.

Bruggi, M., 2008. "On an alternative approach to stress constraints relaxation in topology optimization". *Structural and Multidisciplinary Optimization*, Vol. 36, No. 2, pp. 125–141. ISSN 1615147X. doi:10.1007/s00158-007-0203-6.

Cai, S., Zhou, W., Wei, H. and Zhu, M., 2023. "Topology Optimization Design of Multi-Input-Multi-Output Compliant Mechanisms with Hinge-Free Characteristic and Totally Decoupled Kinematics". *Applied Sciences (Switzerland)*, Vol. 13.

Cardoso, E.L. and Heiden, G., 2023. "Codelenz/walle.jl". doi:10.5281/zenodo.8066166.

Cardoso, E. and Fonseca, J., 2004. "Strain energy maximization approach to the design of fully compliant mechanisms using topology optimization". *Latin American Journal of Solids and Structures*, Vol. 1.

da Silva, G.A., Beck, A.T. and Cardoso, E.L., 2018. "Topology optimization of continuum structures with stress constraints and uncertainties in loading". *International Journal for Numerical Methods in Engineering*, Vol. 113, No. 1, pp. 153–178. doi:https://doi.org/10.1002/nme.5607.

Ding, S., Li, B., Chen, G., Zhao, Z. and Hong, J., 2021. "Isogeometric topology optimization of compliant mechanisms using transformable triangular mesh (TTM) algorithm". *Structural and Multidisciplinary Optimization*, Vol. 64, No. 4, pp. 2553–2576. ISSN 16151488. doi:10.1007/s00158-021-03008-9.

Duysinx, P. and Bendsøe, M.P., 1998. "Topology optimization of continuum structures with local stress constraints". *International Journal for Numerical Methods in Engineering*, Vol. 43, No. 8, pp. 1453–1478. doi: https://doi.org/10.1002/(SICI)1097-0207(19981230)43:8<1453::AID-NME480>3.0.CO;2-2.

Jung, U.J. and Park, G.J., 2015. "A new method for simultaneous optimum design of structural and control systems". *Computers & Structures*, Vol. 160, pp. 90–99. doi:10.1016/j.compstruc.2015.08.006.

Kang, B.S., Choi, W.S. and Park, G.J., 2001. "Structural optimization under equivalent static loads transformed from dynamic loads based on displacement". *Computers & Structures*, Vol. 79, No. 2, pp. 145–154. doi:10.1016/s0045-7949(00)00127-9.

Kirsch, U., 1990. "On singular topologies in optimum structural design". *Structural optimization*, Vol. 2, No. 3, pp. 133–142. ISSN 1615-1488. doi:10.1007/BF01836562.

Kirsch, U., 1989. "Optimal topologies of truss structures". *Computer Methods in Applied Mechanics and Engineering*, Vol. 72, No. 1, pp. 15–28. ISSN 00457825. doi:10.1016/0045-7825(89)90119-9.

Lee, H.A. and Park, G.J., 2015. "Nonlinear dynamic response topology optimization using the equivalent static loads method". *Computer Methods in Applied Mechanics and Engineering*, Vol. 283, pp. 956–970. doi: 10.1016/j.cma.2014.10.015.

Liang, Y., Sun, K. and Cheng, G.D., 2020. "Discrete variable topology optimization for compliant mechanism design via Sequential Approximate Integer Programming with Trust Region (SAIP-TR)". *Structural and Multidisciplinary Optimization*, Vol. 62, No. 6, pp. 2851–2879. ISSN 16151488. doi:10.1007/s00158-020-02693-2.

Lu, Y. and Tong, L., 2021. "Topology optimization of compliant mechanisms and structures subjected to design-dependent pressure loadings". *Structural and Multidisciplinary Optimization*, Vol. 63, No. 4, pp. 1889–1906. ISSN 16151488.

doi:10.1007/s00158-020-02786-y.

Ma, Z.D., Kikuchi, N. and Hagiwara, I., 1993. "Structural topology and shape optimization for a frequency response problem". *Computational Mechanics*, Vol. 13, No. 3, pp. 157–174. ISSN 01787675. doi:10.1007/BF00370133.

Min, S., Kikuchi, N., Park, Y.C., Kim, S. and Chang, S., 1999. "Optimal topology design of structures under dynamic loads". *Structural Optimization*, Vol. 17, No. 2, pp. 208–218. ISSN 09344373. doi:10.1007/s001580050052.

Miyajima, K., Noguchi, Y. and Yamada, T., 2022. "Optimal design of compliant displacement magnification mechanisms using stress-constrained topology optimization based on effective energy". doi:10.1016/j.finel.2022.103892.

Montero, D.S., Silva, O.M. and Cardoso, E.L., 2019. "Topology optimization for harmonic vibration problems using a density-weighted norm objective function". doi:10.1007/s00158-020-02695-0.

Montero, D.S., Silva, O.M. and Cardoso, E.L., 2020. "Topology optimization for harmonic vibration problems using a density-weighted norm objective function". *Structural and Multidisciplinary Optimization*, Vol. 62, No. 6, pp. 3301–3327. ISSN 16151488. doi:10.1007/s00158-020-02695-0.

Nejat, Ali; Held, Alexander; Seifried, R., 2022. "A comparasion of a level set method and the method of moving asymptotes for the topology optimization of flexible components in multibody systems". doi:10.1002/pamm.202200103.

Neves, M.M., Rodrigues, H. and Guedes, M., 1995. "Technical Papers Generalized topology criterion design of structures with a buckling load". *Structural Optimization*, Vol. 10, pp. 71–78.

Olhoff, N. and Du, J., 2008. "On topological design optimization of structures against vibration and noise emission". In *Computational Aspects of Structural Acoustics and Vibration*, Springer, pp. 217–276.

Park, G.J., 2010. "Technical overview of the equivalent static loads method for non-linear static response structural optimization". *topology optimization to minimize the dynamic compliance ofltidisciplinary Optimization*, Vol. 43, No. 3, pp. 319–337. doi:10.1007/s00158-010-0530-x.

Pereira, A. and Cardoso, E.L., 2018. "On the influence of local and global stress constraint and filtering radius on the design of hinge-free compliant mechanisms". *Structural and Multidisciplinary Optimization*, Vol. 58, No. 2, pp. 641–655. ISSN 16151488. doi:10.1007/s00158-018-1915-5.

Shu, L., Wang, M.Y., Fang, Z., Ma, Z. and Wei, P., 2011. "Level set based structural topology optimization for minimizing frequency response". *Journal of Sound and Vibration*, Vol. 330, No. 24, pp. 5820–5834. ISSN 0022460X. doi:10.1016/j.jsv.2011.07.026.

Silva, O.M., 2017. *Otimização Topológica em Problemas de Vibrações Harmônicas Utilizando Potência de Entrada*. Doctorate thesis, Universidade Federal de Santau Catarina.

Svéd, G. and Ginos, Z., 1968. "Structural optimization under multiple loading". *International Journal of Mechanical Sciences*, Vol. 10, pp. 803–805.

Tcherniak, D., 1999. "Topology optimization of resonating structures using SIMP method". *International Journal for Numerical Methods in Engineering*, Vol. 54, No. 11, pp. 1605–1622. ISSN 00295981. doi:10.1002/nme.484.

Valentini, F., Silva, O.M. and Cardoso, E.L., 2021. "Robust topology optimization for harmonic displacement minimization of structures subjected to uncertainty in the excitation frequency". *Computer Methods in Applied Mechanics and Engineering*, Vol. 379, p. 113767. ISSN 0045-7825. doi:https://doi.org/10.1016/j.cma.2021.113767.

Venini, P., 2016. "Dynamic compliance optimization". *Computers & Structures*, Vol. 177, pp. 12–22. doi:10.1016/j.compstruc.2016.07.012.

Wang, F., Lazarov, B.S. and Sigmund, O., 2011. "On projection methods, convergence and robust formulations in topology optimization". *Structural and Multidisciplinary Optimization*, Vol. 43, No. 6, pp. 767–784. ISSN 16151488. doi:10.1007/s00158-010-0602-y.

Yang, X. and Li, Y., 2012. "Topology optimization to minimize the dynamic compliance of a bi-material plate in a thermal environment". *topology optimization to minimize the dynamic compliance ofltidisciplinary Optimization*, Vol. 47, No. 3, pp. 399–408. doi:10.1007/s00158-012-0831-3.

Yang, X. and Li, Y., 2013. "Structural topology optimization on dynamic compliance at resonance frequency in thermal environments". *topology optimization to minimize the dynamic compliance ofltidisciplinary Optimization*, Vol. 49, No. 1, pp. 81–91. doi:10.1007/s00158-013-0961-2.

Zhu, B., Zhang, X., Zhang, H., Liang, J., Zang, H., Li, H. and Wang, R., 2020. "Design of compliant mechanisms using continuum topology optimization: A review". *Mechanism and Machine Theory*, Vol. 143. ISSN 0094114X. doi:10.1016/j.mechmachtheory.2019.103622.

Zhu, M., Yang, Y., Guest, J.K. and Shields, M.D., 2017. "Topology optimization for linear stationary stochastic dynamics". *Structural Safety*, Vol. 67, pp. 116–131. doi:10.1016/j.strusafe.2017.04.004.

8. RESPONSIBILITY NOTICE

The authors are solely responsible for the printed material included in this paper.